Gas Detectors

F.Sauli, Principles of operation of multiwire proportional chambers

https://cds.cern.ch/record/117989/files/CERN-77-09.pdf

Properties of several gases used in proportional counters (from different sources, see the bibliography for this section). Energy loss and ion pairs per unit length are given at atmospheric pressure for minimum ionizing particles

Gas	Z	A	δ (g/cm^3)	E_{ex}	E_i (eV)	I_0 (eV)	W_i	dE/dx ($MeV/g\ cm^{-2}$)	dE/dx (keV/cm)	n_p (i.p./cm) a)	n_T (i.p./cm) a)
H_2	2	2	8.38×10^{-5}	10.8	15.9	15.4	37	4.03	0.34	5.2	9.2
He	2	4	1.66×10^{-4}	19.8	24.5	24.6	41	1.94	0.32	5.9	7.8
N_2	14	28	1.17×10^{-3}	8.1	16.7	15.5	35	1.68	1.96	(10)	56
O_2	16	32	1.33×10^{-3}	7.9	12.8	12.2	31	1.69	2.26	22	73
Ne	10	20.2	8.39×10^{-4}	16.6	21.5	21.6	36	1.68	1.41	12	39
Ar	18	39.9	1.66×10^{-3}	11.6	15.7	15.8	26	1.47	2.44	29.4	94
Kr	36	83.8	3.49×10^{-3}	10.0	13.9	14.0	24	1.32	4.60	(22)	192
Xe	54	131.3	5.49×10^{-3}	8.4	12.1	12.1	22	1.23	6.76	44	307
CO_2	22	44	1.86×10^{-3}	5.2	13.7	13.7	33	1.62	3.01	(34)	91
CH_4	10	16	6.70×10^{-4}		15.2	13.1	28	2.21	1.48	16	53
C_4H_{10}	34	58	2.42×10^{-3}		10.6	10.8	23	1.86	4.50	(46)	195

a) i.p. = ion pairs

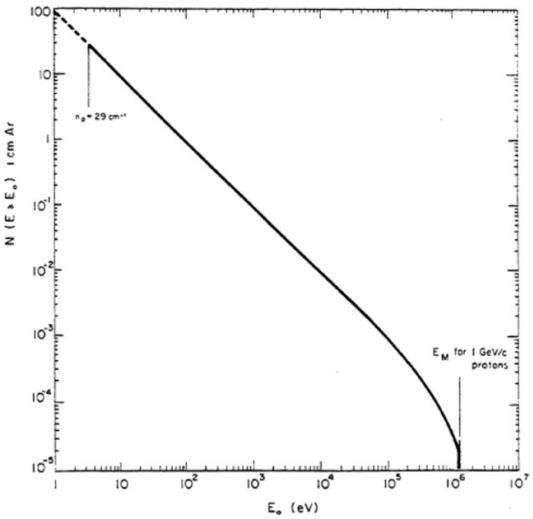

Fig. 4 Computed number of δ electrons ejected at an energy larger than or equal to E_0, as a function of E_0, in 1 cm of argon at normal conditions. The average number of primary ionizing collisions (29 per cm) and the maximum allowed energy transfer for 1 GeV/c protons are shown.

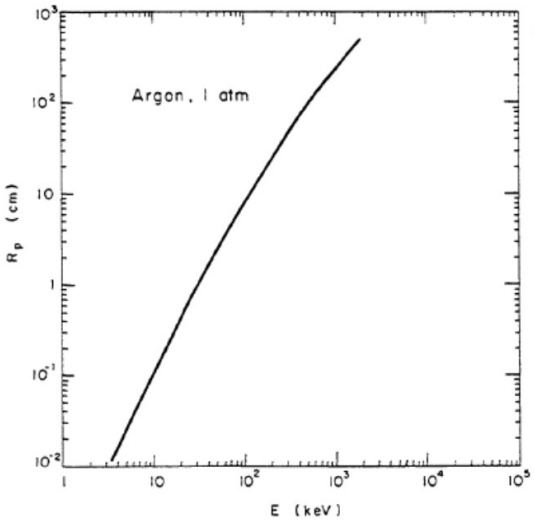

J. 5 Range of electrons in argon, at normal conditions as a function of energy, deduced from measurement in light materials[8])

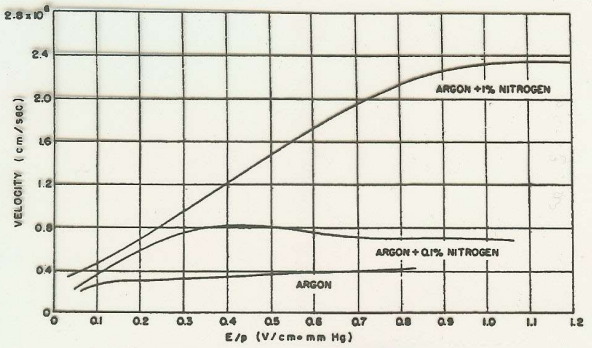

Fig. 25 Drift velocity of electrons in [illegible] argon, and in argon with small added quantities of nitrogen. The very large effect on the velocity for small additions is apparent[22]).

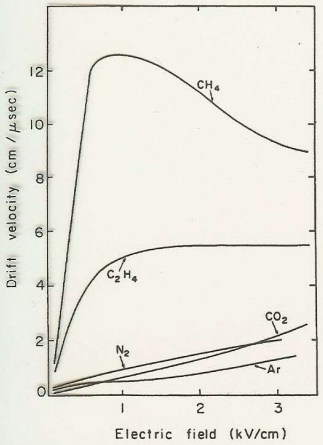

Fig. 26 Drift velocity of electrons in several gases at normal conditions[12,22,23])

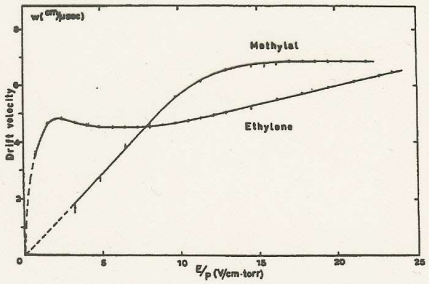

Fig. 27 Drift velocity of electrons in methylal $[(OCH_3)_2CH_2]$ and in ethylene (C_2H_4) [24])

CHARGE TRANSPORT DETERMINED BY ELECTRON-MOLECULE CROSS SECTION:

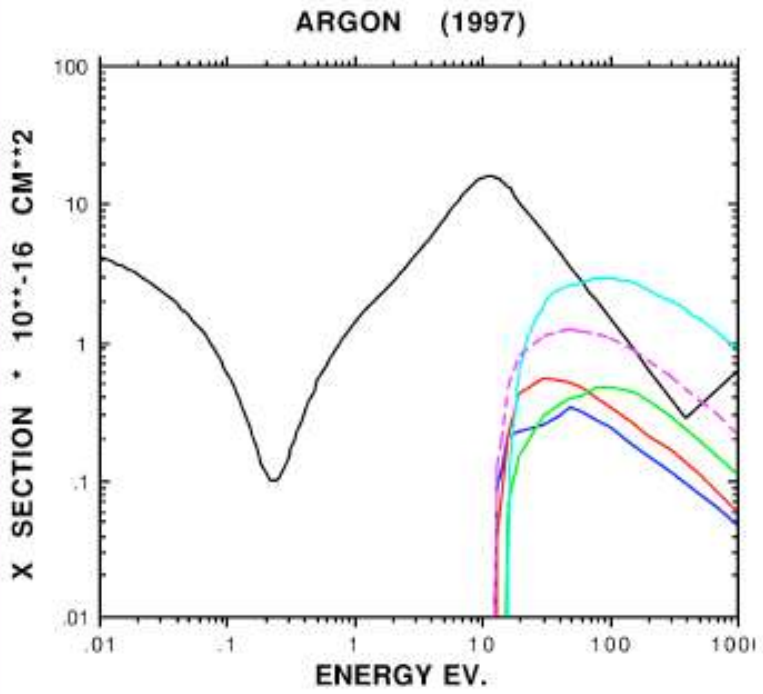

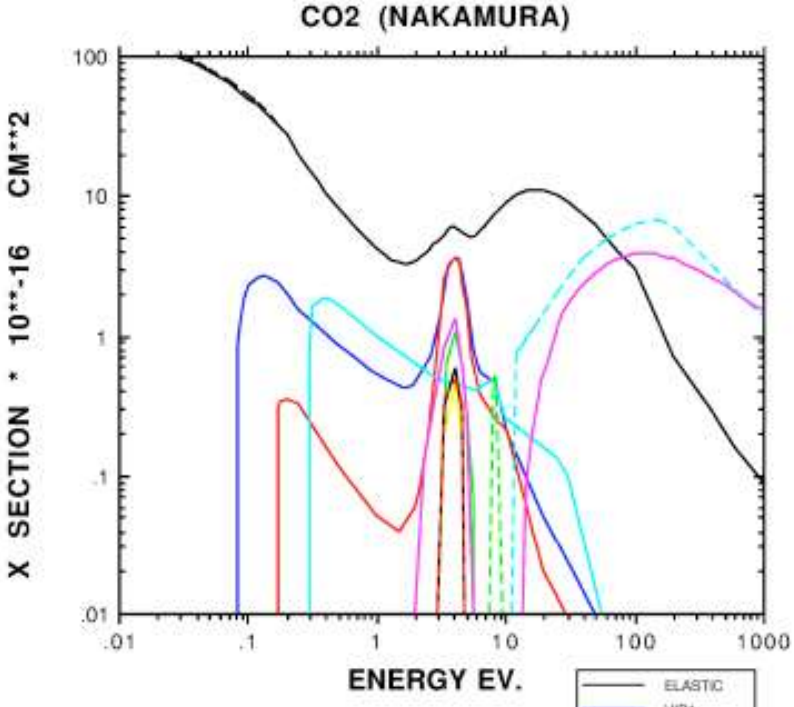

MAGBOLTZ

S. Biagi, Nucl. Instr. and Meth. A421 (1999) 234

http://consult.cern.ch/writeup/magboltz/cross/

http://cpa94.ups-tlse.fr/operations/operation_03/POSTERS/BOLSIG/

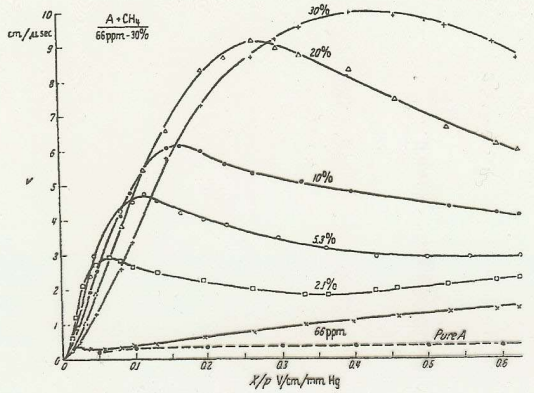

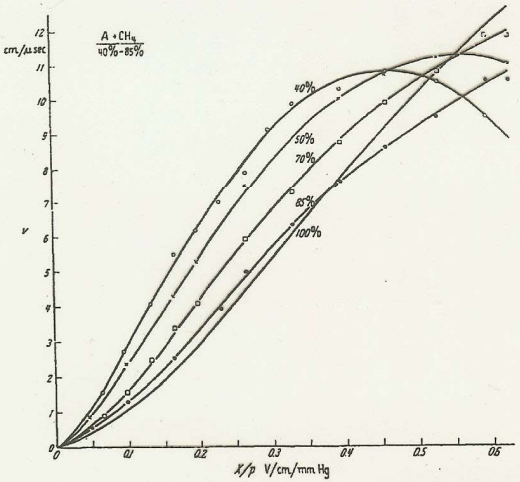

Fig. 28 Drift velocity of electrons in several argon-methane mixtures[12])

LARGE RANGE OF DRIFT VELOCITIES AND DIFFUSIONS

DRIFT VELOCITY:

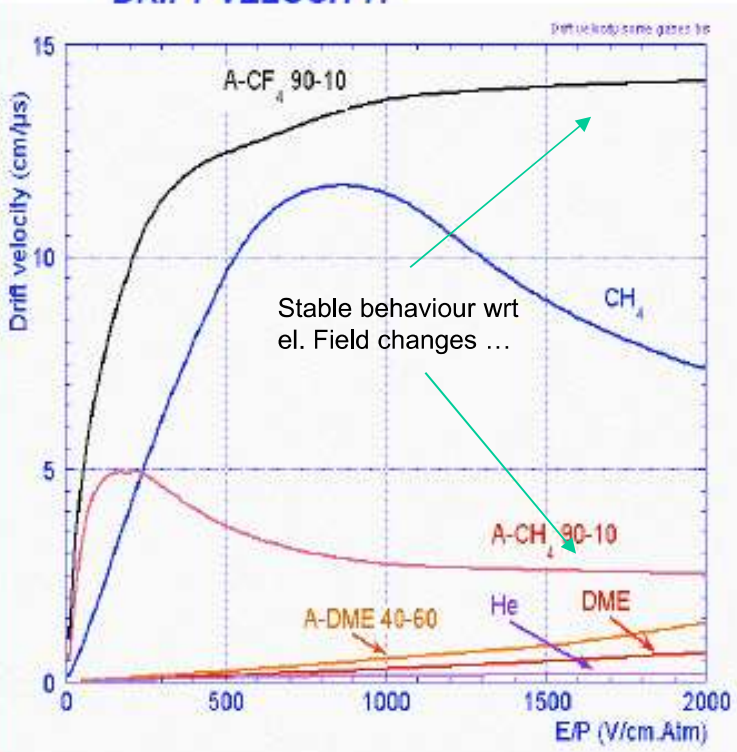

DIFFUSION:

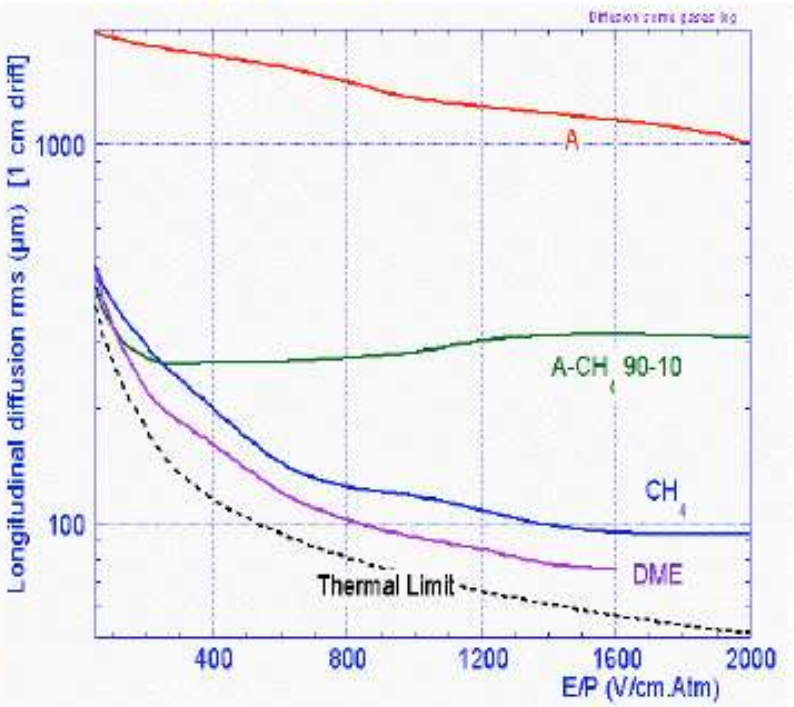

COMPUTED DRIFT VELOCITY IN MIXTURES

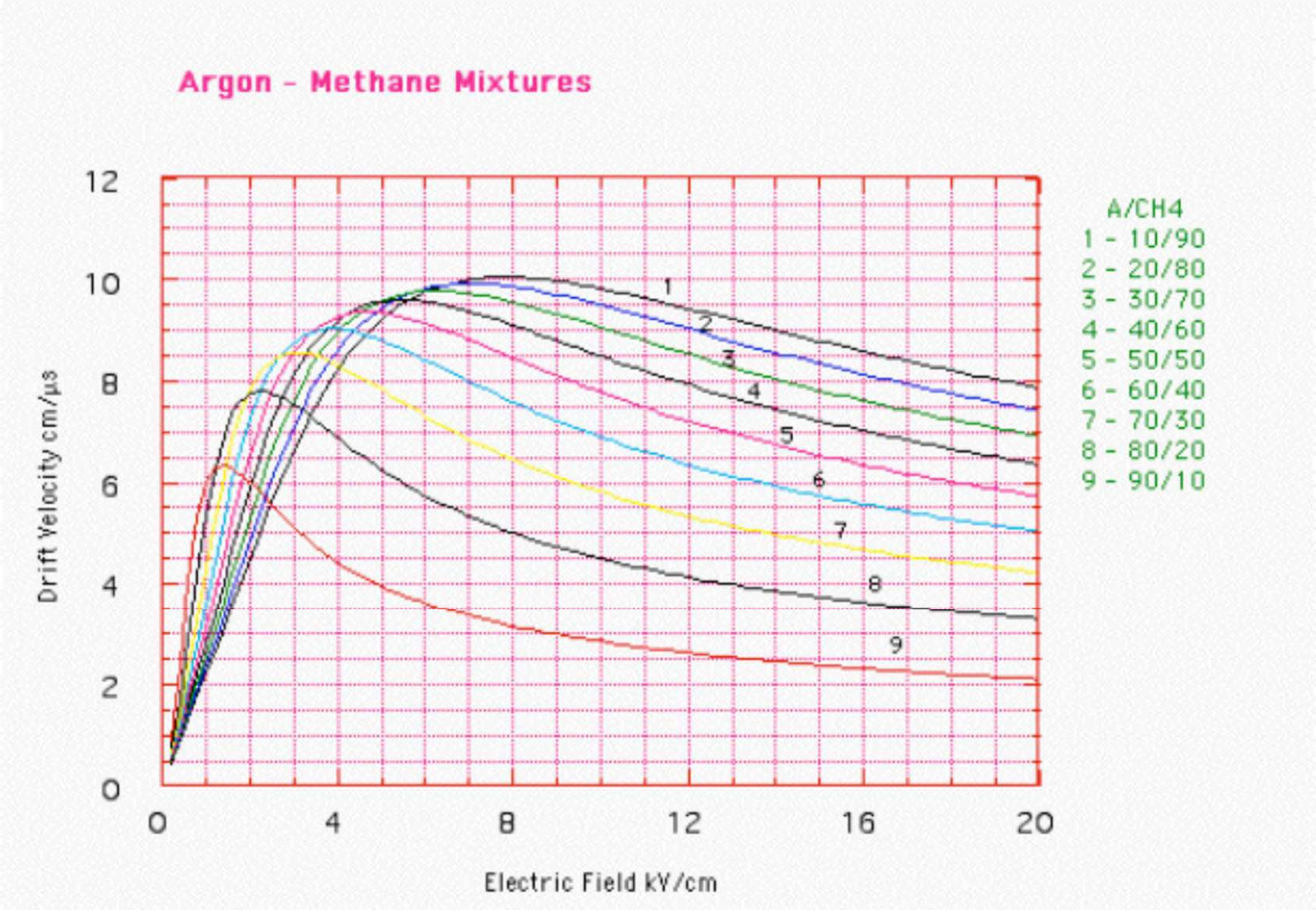

http://consult.cern.ch/writeup/garfield/examples/gas/trans2000.html#elec

Velocita' di deriva degli elettroni

Velocita' di deriva in una miscela $Ar/CO_2/CF_4$ (60/20/20).

Satura a

$w^- \approx 10$ cm/μs
$\Rightarrow$100 μm/ns

3000 volte la velocita' degli ioni

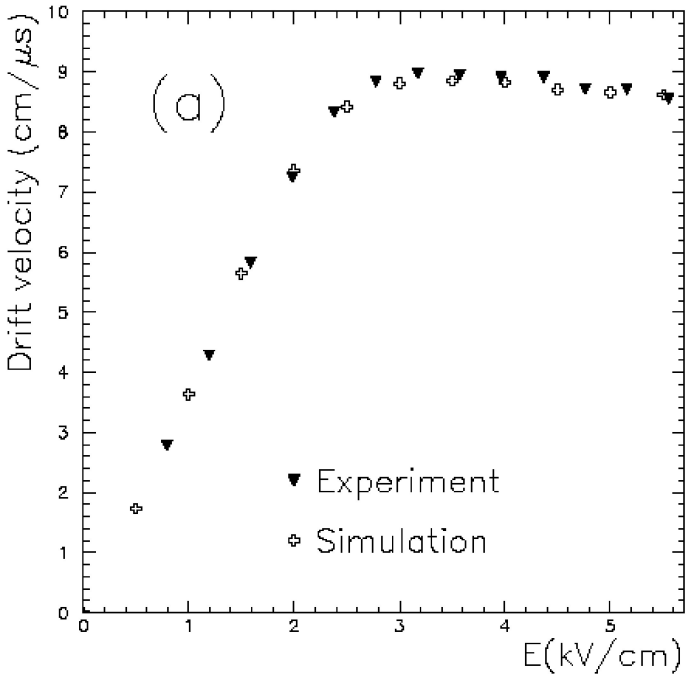

ELECTRON TRANSPORT THEORY

BALANCE BETWEEN ENERGY ACQUIRED FROM THE FIELD AND COLLISION LOSSES

Energy distribution probability:

$$F_0(\varepsilon) = C\sqrt{\varepsilon}\; e^{-\int \frac{3\varepsilon\,\Lambda(\varepsilon)\,d\varepsilon}{[e\,E\,l_e(\varepsilon)]^2}}$$

$$l_e(\varepsilon) = \frac{1}{N\,\sigma(\varepsilon)}$$

Mean free path between collisions

(σ : electron-molecule cross section)

$\Lambda(\varepsilon)$ *Fractional energy loss in collisions*

Drift velocity:

$$w = \frac{2}{3}\frac{e}{m} E \int \varepsilon\, l_e(\varepsilon) \frac{\partial \dfrac{F_0(\varepsilon)}{\nu}}{\partial\varepsilon} d\varepsilon \qquad v = \sqrt{\frac{2\varepsilon}{m}}$$

Diffusion coefficient:

$$D = \int \frac{l_e(\varepsilon)}{3}\, v\, F_0(\varepsilon)\, d\varepsilon$$

Frost and Phelps, Phys. Rev. 127(1962)1621
V. Palladino and B. Sadoulet, Nucl. Instr. and Meth. 128(1975)323
G. Shultz and J. Gresser, Nucl. Instr. and Meth. 151(1978)413
S. Biagi, Nucl. Instr. and Meth. A283(1989)716

Deriva e diffusione degli elettroni

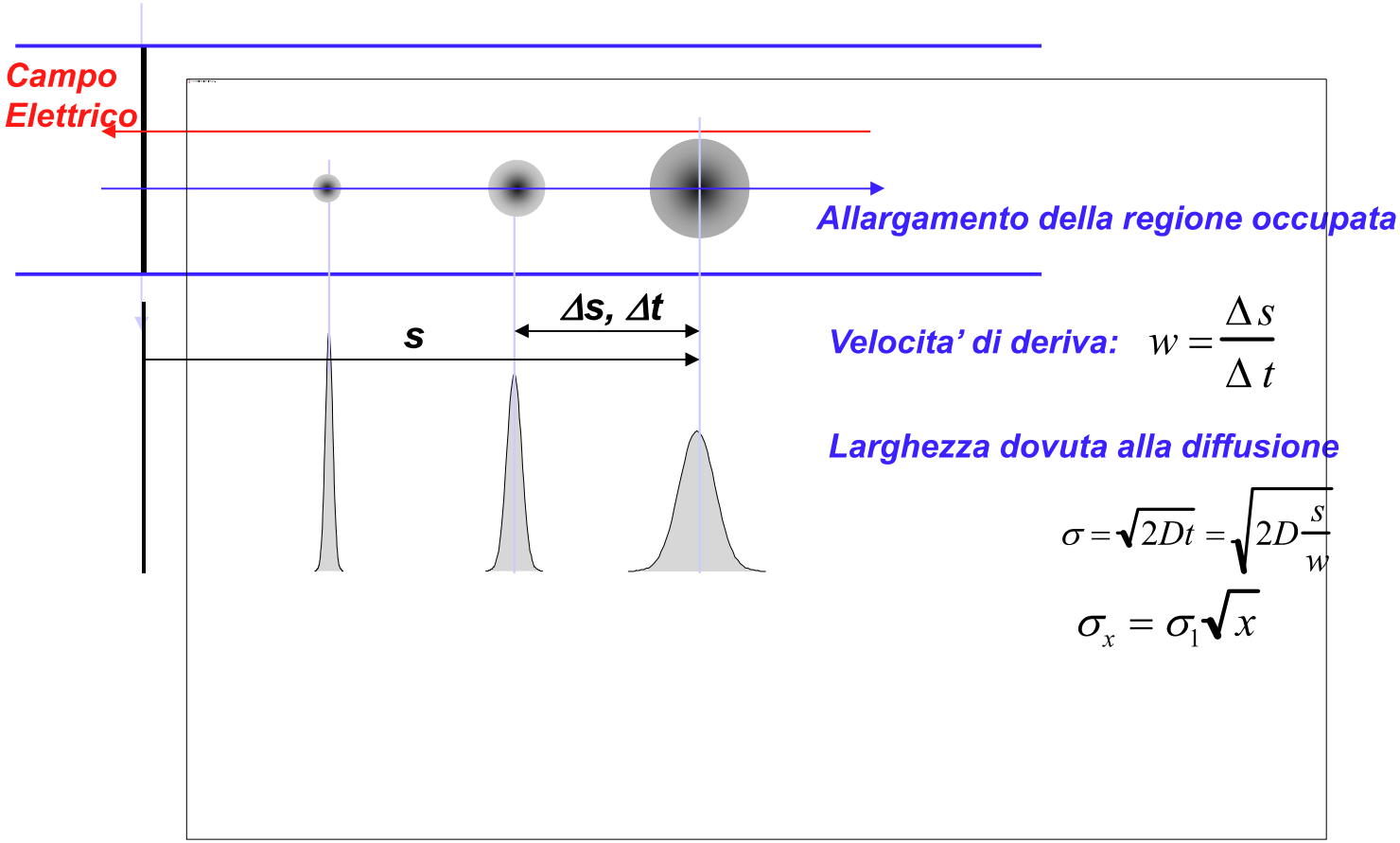

Velocita' di deriva: $w = \frac{\Delta s}{\Delta t}$

Larghezza dovuta alla diffusione

$$\sigma = \sqrt{2Dt} = \sqrt{2D\frac{s}{w}}$$

$$\sigma_x = \sigma_1 \sqrt{x}$$

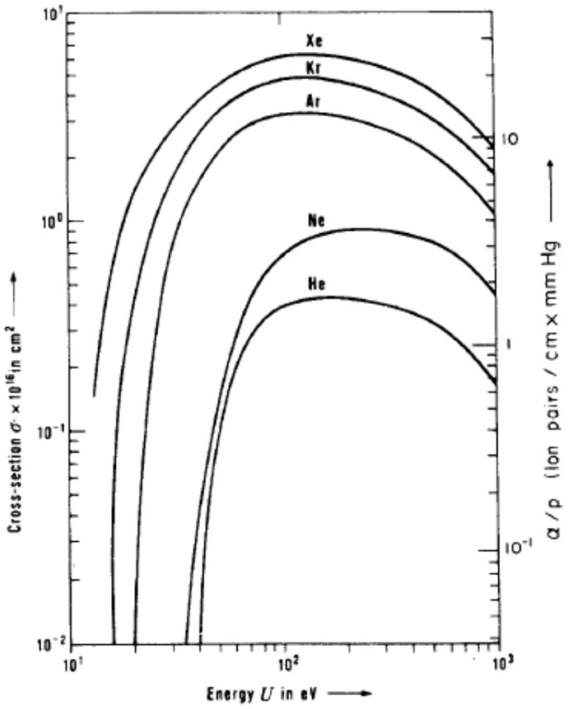

Fig. 45 Cross-section and first Townsend coefficient as a function of electron energy, for noble gases[28]

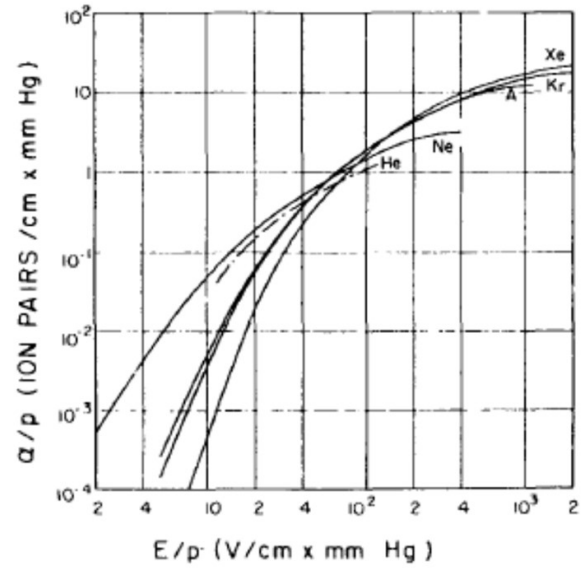

Fig. 44 First Townsend coefficient as a function of the reduced electric field, for noble gases[22]

TOWNSEND COEFFICIENT IN GAS MIXTURES ARGON-CH_4:

T.C. dependence on gas mixture

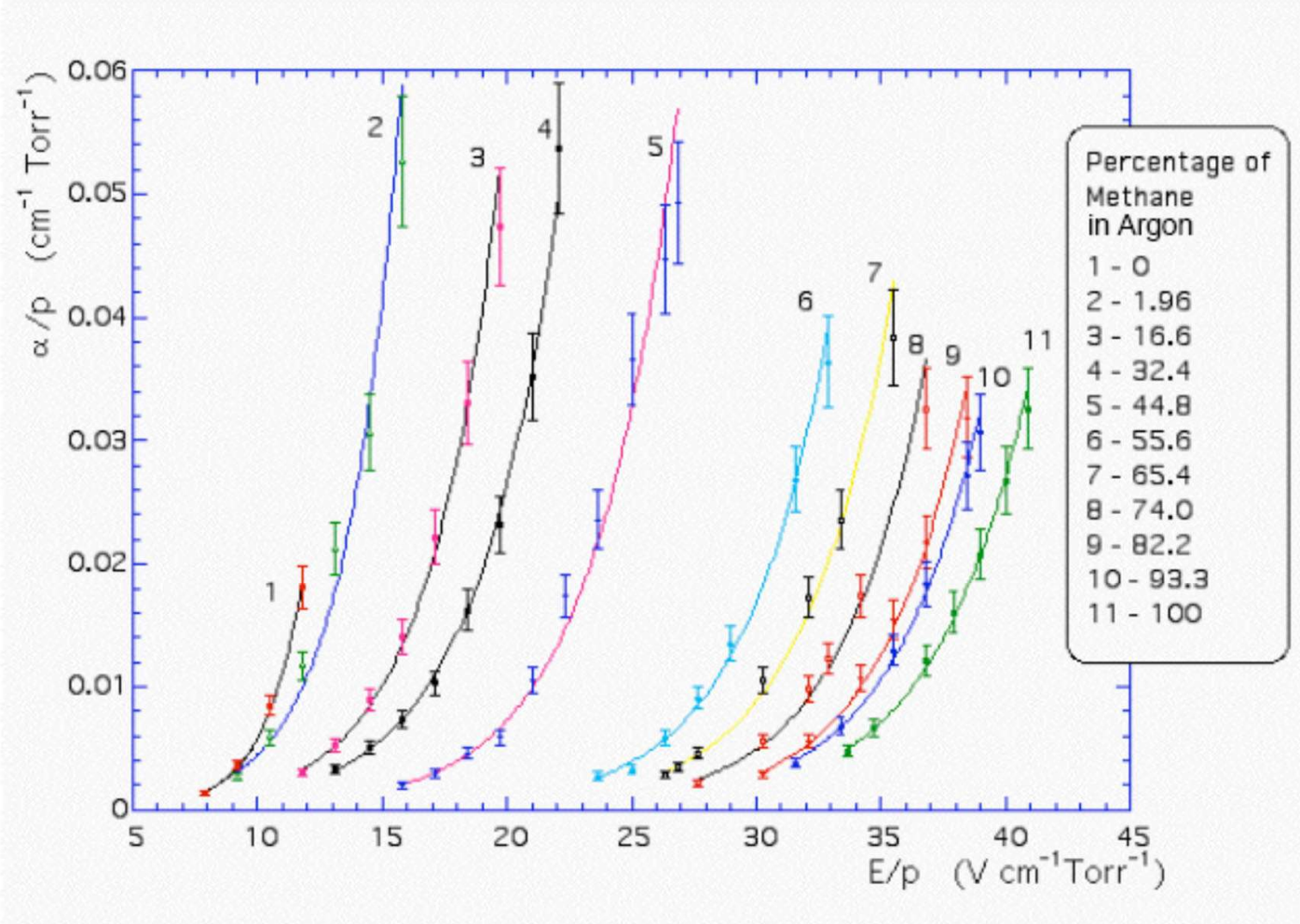

AVALANCHE MULTIPLICATION IN UNIFORM FIELD

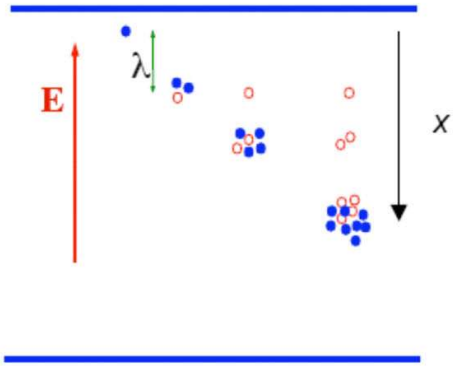

$$dn = n\,\alpha\,dx$$

$$n(x) = n_0 e^{\alpha x}$$

Multiplication factor or Gain

$$M(x) = \frac{n}{n_0} = e^{\alpha x}$$

Combined cloud chamber-avalanche chamber:

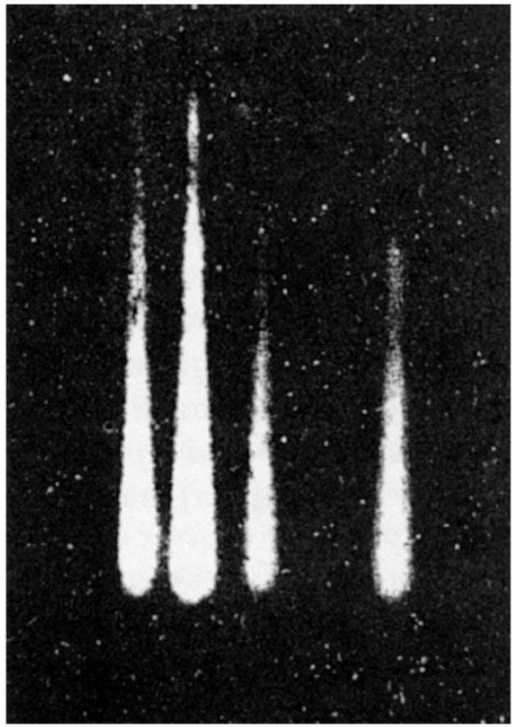

H. Raether
Electron avalanches and breakdown in gases
(Butterworth 1964)

Signal development around the anode radius

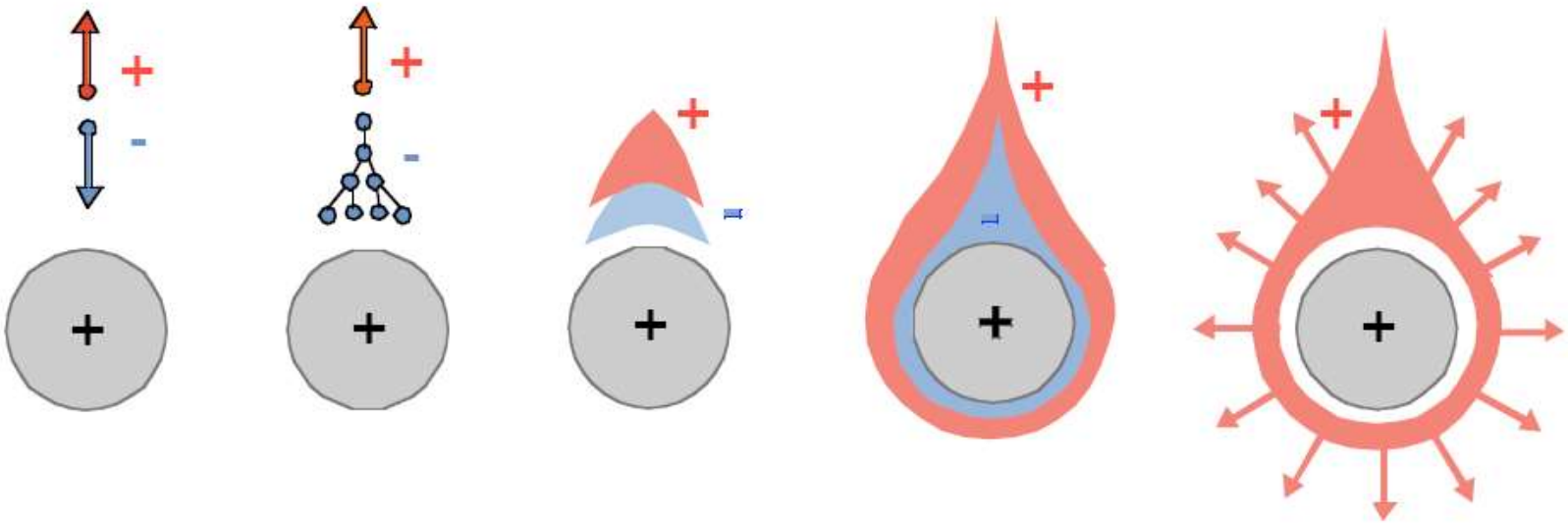

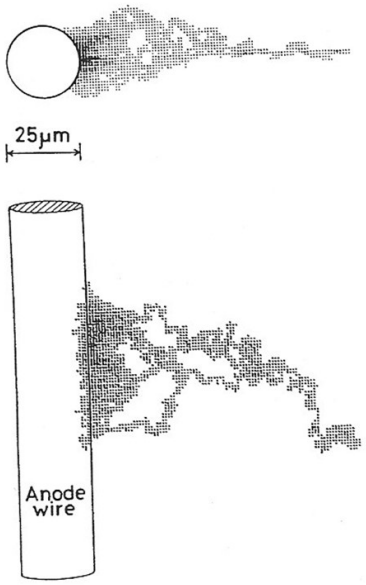

Figure 6.5 Orthogonal views of an avalanche triggered by a single electron as simulated by a Monte Carlo calculation. The density of the shading indicates the concentration of electrons formed in the avalanche. (From Matoba et al.[3])

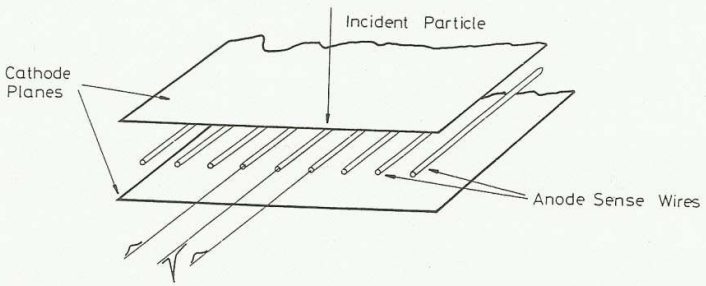

Fig. 6.7. Basic configuration of a multiwire proportional chamber. Each wire acts as an independent proportional counter. The signal on the firing wire is negative while the signals on the neighboring wires are small and positive

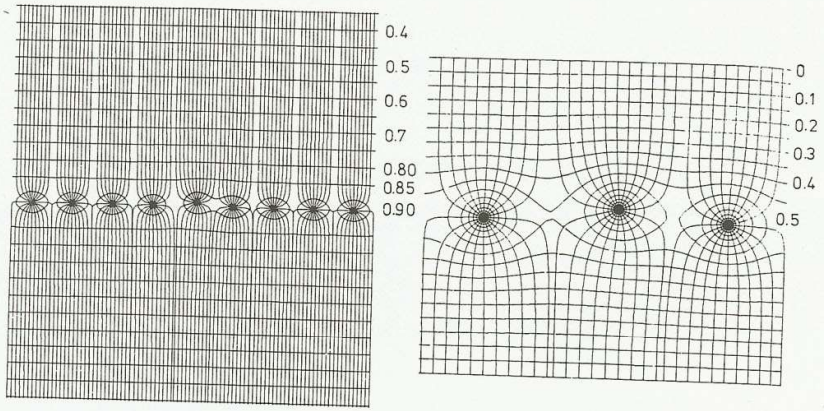

Fig. 6.8. Electric field lines and potentials in a multiwire proportional chamber. The effect of a slight v displacement on the field lines is also shown (from *Charpak* et al. [6.16])

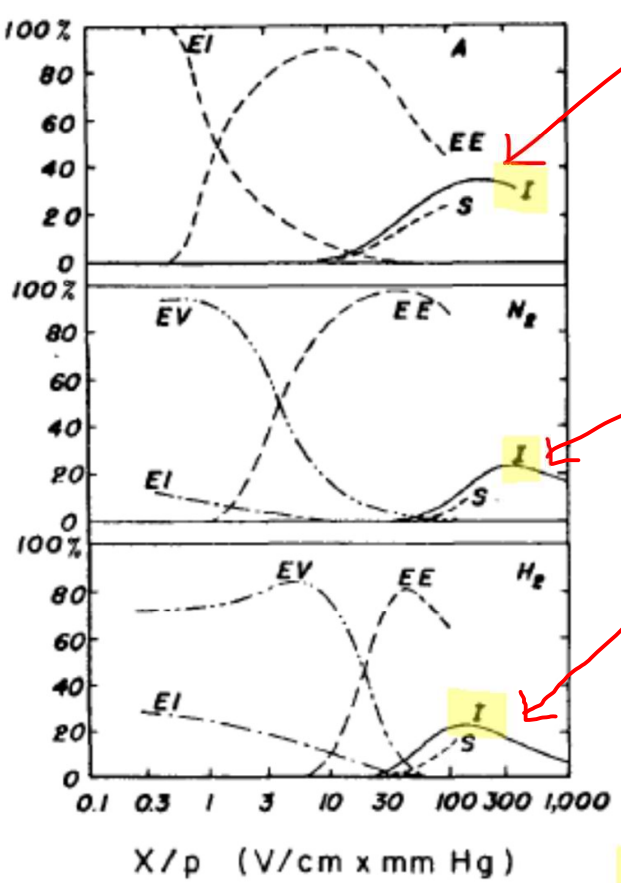

Fig. 43

Approximate curves showing the fraction of energy going into different processes in argon, nitrogen and hydrogen as a function of the reduced electric field[18]. In the figure, El represents the elastic impacts, EV the vibrational excitations, EE the excitations leading to photon emission and I the ionizations.

Strong field only around anode wires

Electrostatic potential in a planar MWPC given by:

$$V(x,y) = -\frac{q}{4\pi\varepsilon_0}\ln\left\{4\left[\sin^2\left(\frac{\pi x}{d}\right) + \sinh^2\left(\frac{\pi y}{d}\right)\right]\right\}$$

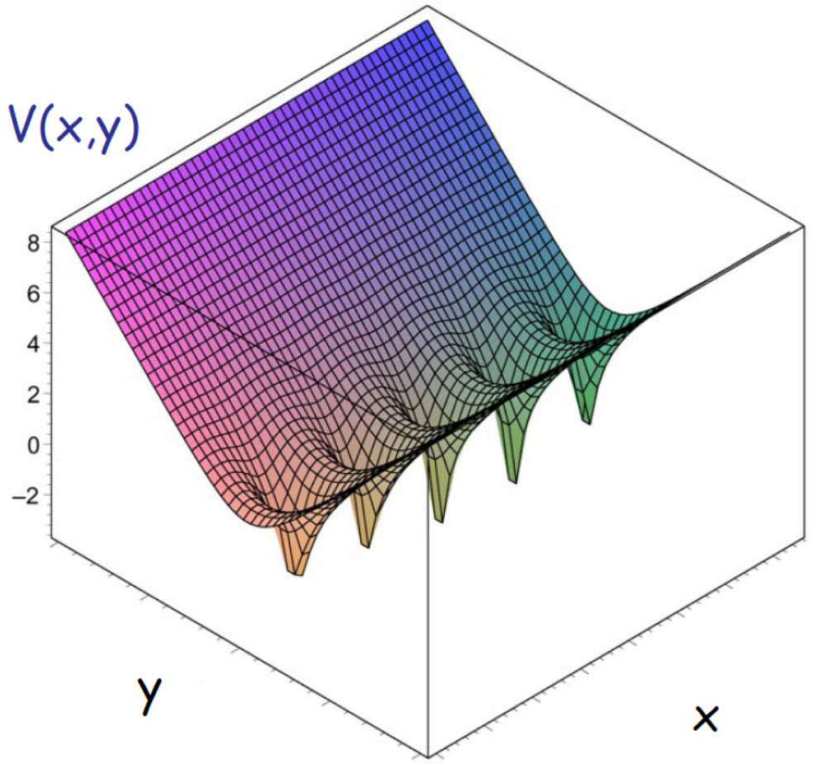

Strong field only around anode wires

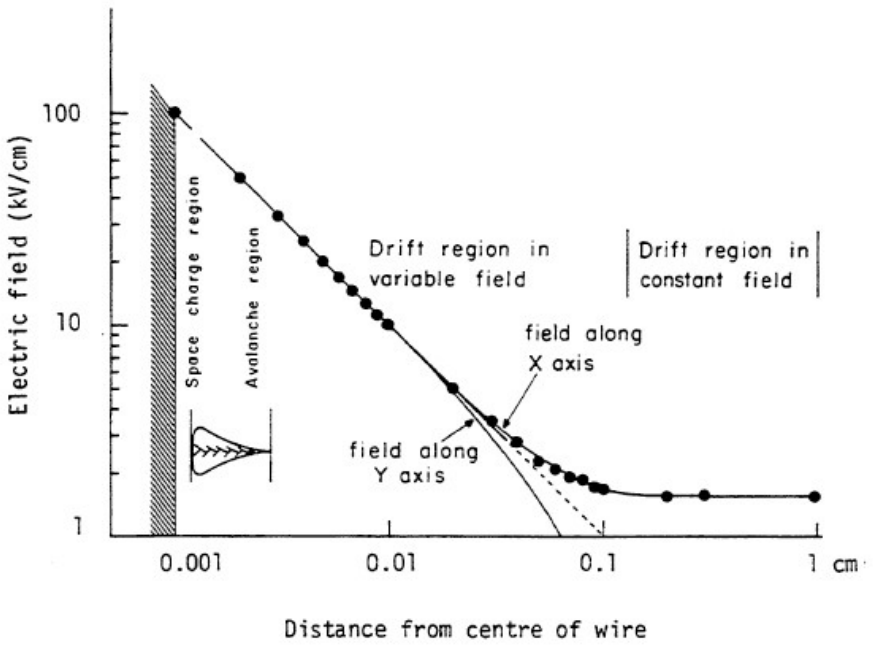

• **scelta dei parametri**

– la camera è tanto più stabile quanto più il filo è sottile

• ragioni meccaniche limitano ad a=20μm a meno di camere molto piccole

– la spaziatura minima dei fili è 2mm

• valori inferiori tendono ad essere instabili elettricamente

• NB al diminuire di s diminuisce C e quindi il campo elettrico a parità di V0

- Stabilità meccanica
  - variazioni percentuali di guadagno causate da problemi meccanici:

ricordando che

$$M \propto e^{CV_0} = e^{Q} \rightarrow \frac{\Delta M}{M} = \Delta Q \rightarrow \frac{\Delta M}{M} = \ln M \cdot \frac{\Delta Q}{Q}$$

dalla capacità per unità di lunghezza a V_0 costante:

$$\frac{\Delta Q}{Q} = \frac{C'}{2\pi\varepsilon_0}\frac{\Delta a}{a} \qquad \frac{\Delta Q}{Q} = \frac{C'b}{2\pi\varepsilon_0 s}\frac{\Delta b}{b}$$

per valori tipici dei parametri:

$$\frac{\Delta M}{M} = 3\frac{\Delta a}{a} \qquad \frac{\Delta M}{M} = 12\frac{\Delta b}{b} \qquad \frac{\Delta M}{M} = 20\frac{\Delta s}{s}$$

  - è necessaria un'ottima precisione costruttiva e stabilità meccanica per avere guadagno uniforme
    - essenziale per misure di energia
  - importanti soprattutto le forze elettrostatiche tra i fili

- Lettura catodica
  - catodo segmentato ortogonalmente ai fili
    - in genere larghezza delle strip ≈ spaziatura anodo-catodo
  - si legge il segnale indotto sul catodo, che interessa più strips adiacenti

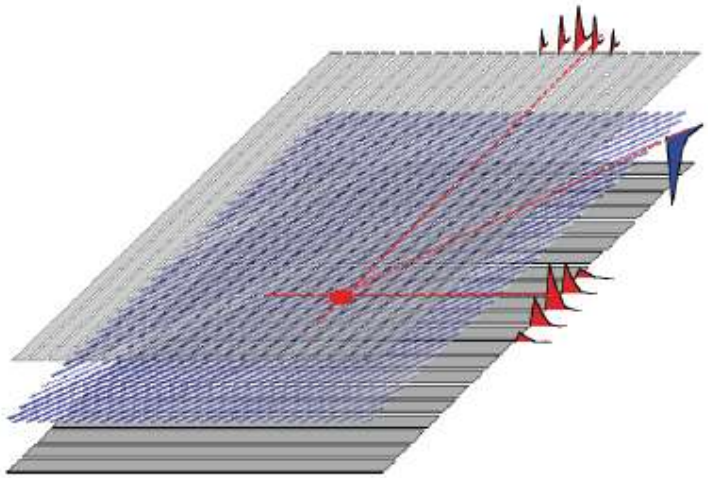

Drift chambers

risoluzione nelle camere a deriva

- tre effetti importanti
  - il rumore dell'elettronica
  - la diffusione longitudinale della carica
    - proporzionale a √t e quindi a √x per velocità di deriva costanti
  - la statistica di ionizzazione primaria

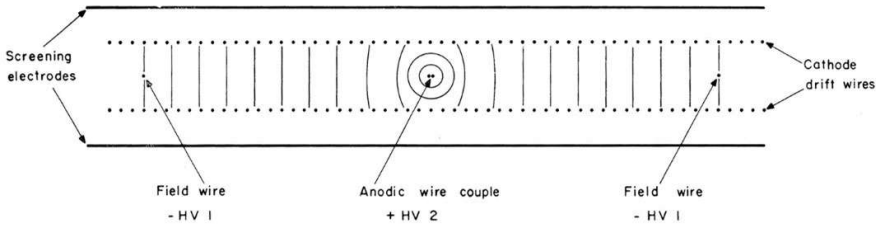

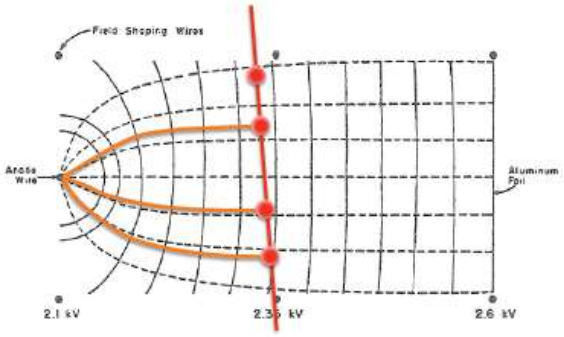

- i percorsi di deriva dei clusters di ioni sono diversi a seconda della posizione lungo la traccia
- effetto rilevante soprattutto per tracce vicine all'anodo

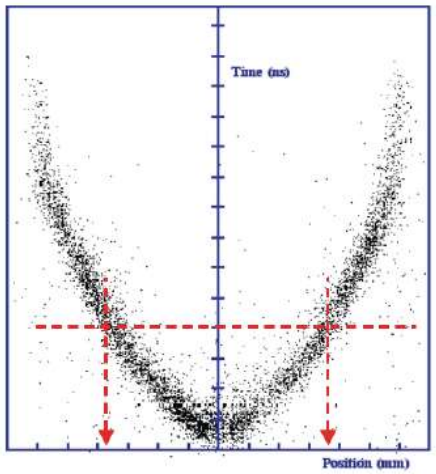

Left-right ambiguity

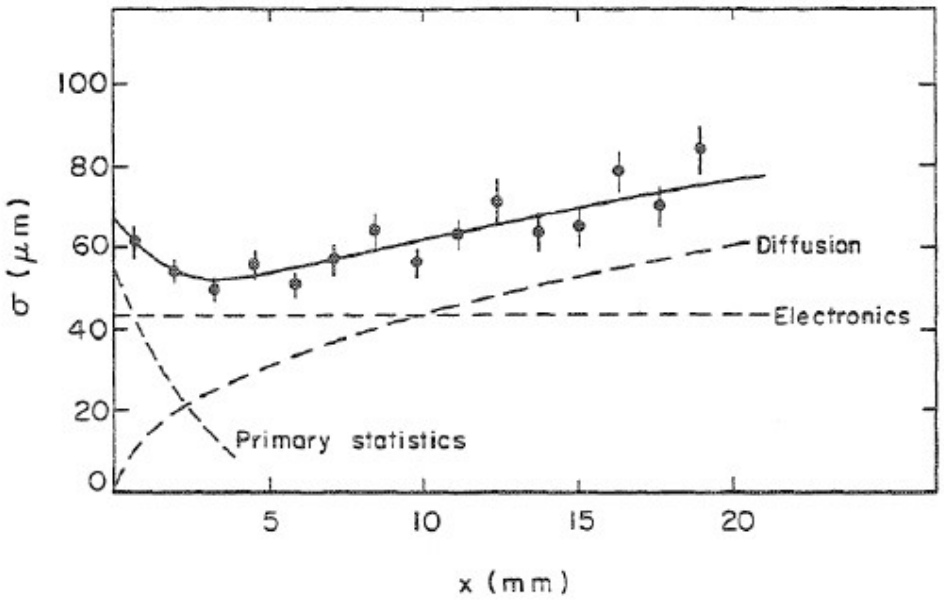
100
80
60
40
20
0
σ (μm)
5
10
15
20
x (mm)
Diffusion
Electronics
Primary statistics

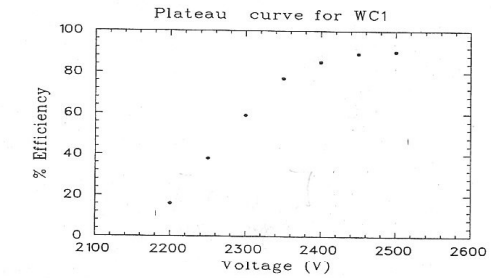

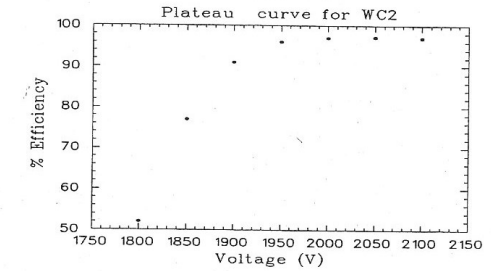

Efficiency vs. voltage (gain)

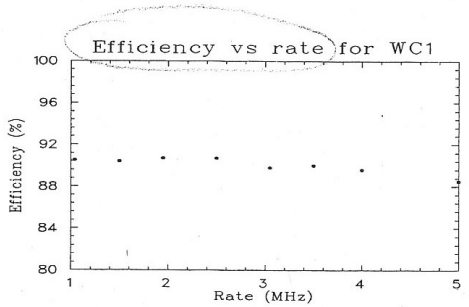

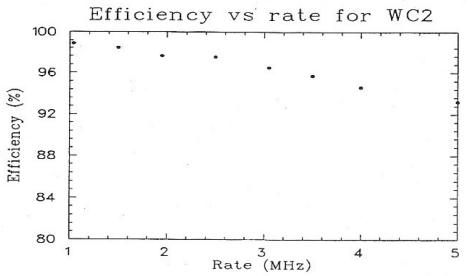

Efficiency vs. rate

Figure 3.6: The efficiency of WC1 and WC2 as a function of the incident beam rate is shown for operating voltages of 2450 V for WC1 and 2050 V for WC2, acquired with 225 MeV/c π^-.

MWPC applications: example of interaction vertex→tgt reconstruction

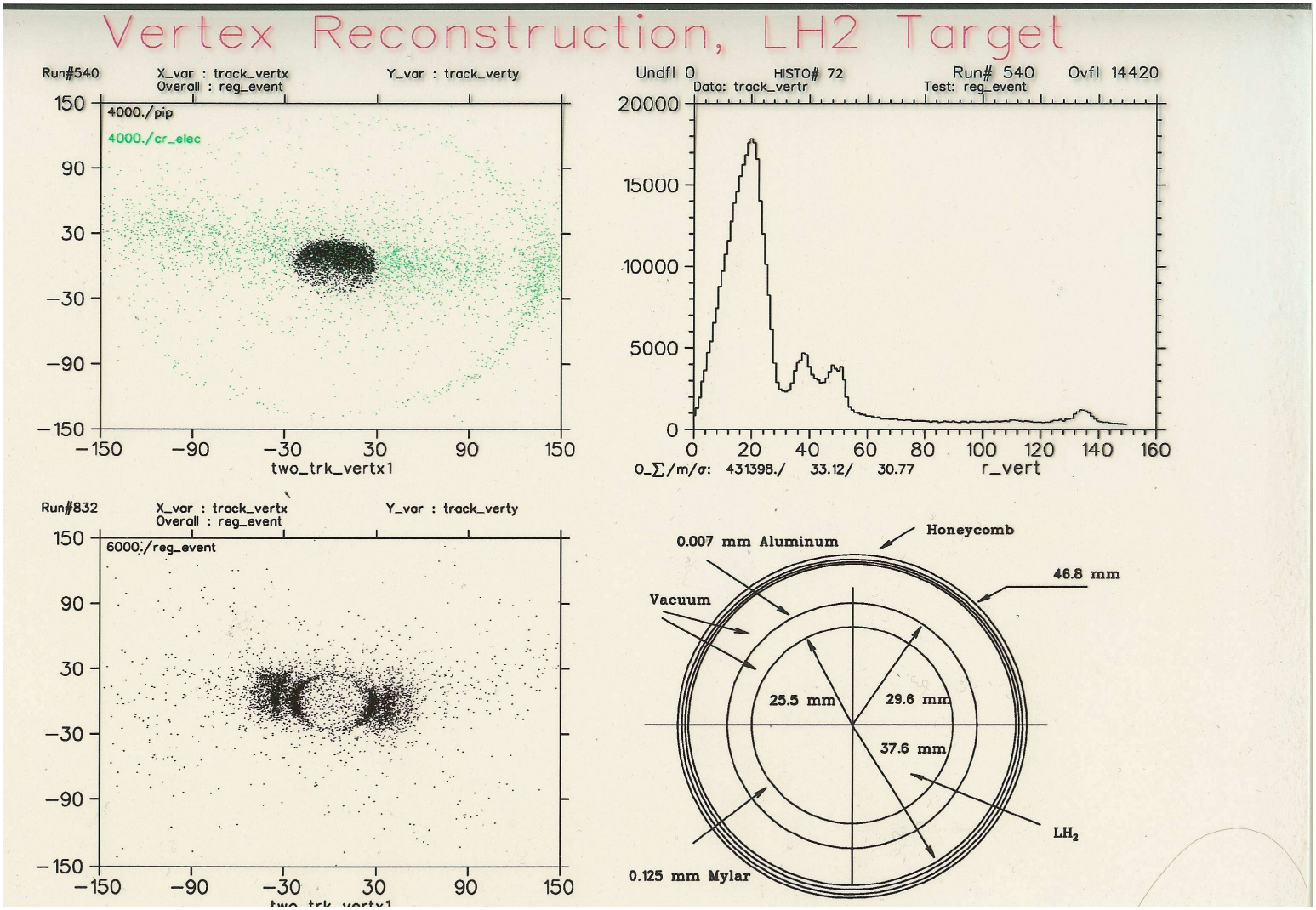

Start with Drift Chambers

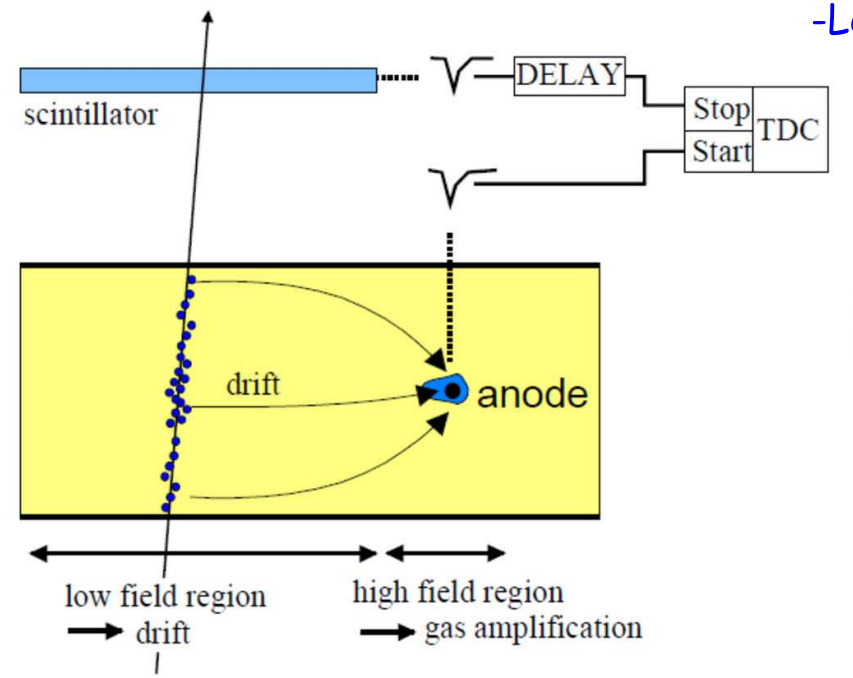

Less wires than in a MWPC➔
-Less electrostatic repulsion between wires (easier mechanics !)
-Less electronics

Resolution not limited by pitch

Measure the arrival time on wire

$$x = v_d (t - t_0)$$

Problems:
Resolution limited by thermal diffusion

Calibration of a Drift Chamber

Position vs. time

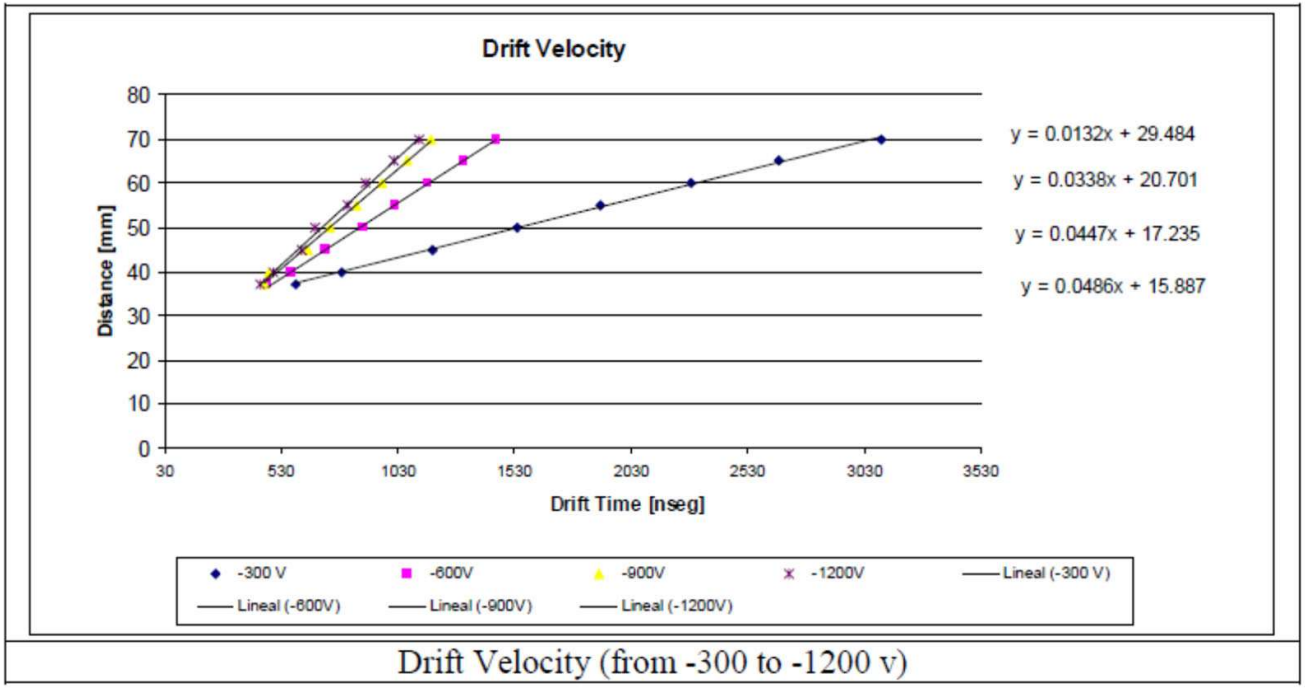

Drift Velocity (from -300 to -1200 v)

DRIFT TIME ACCURACY: DEPENDS ON IONIZATION DENSITY

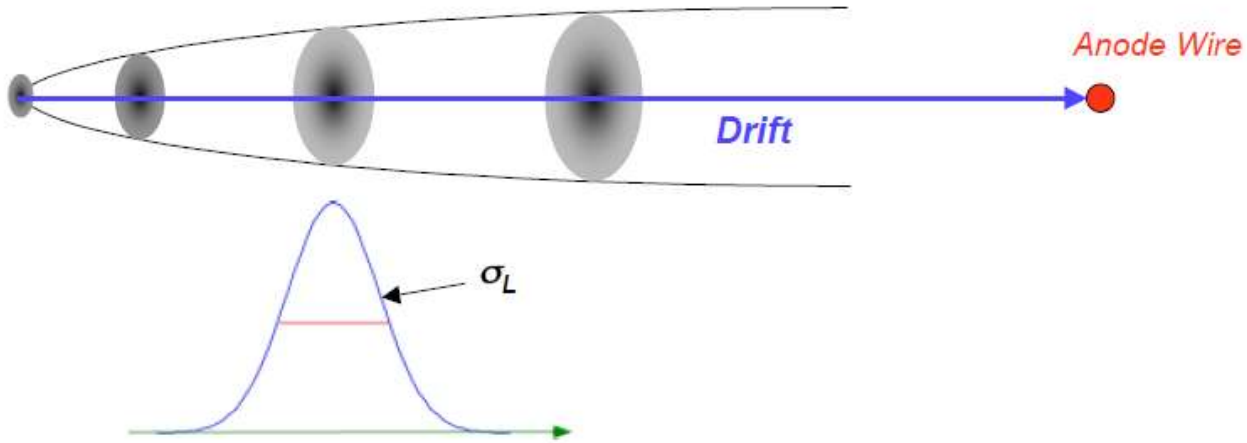

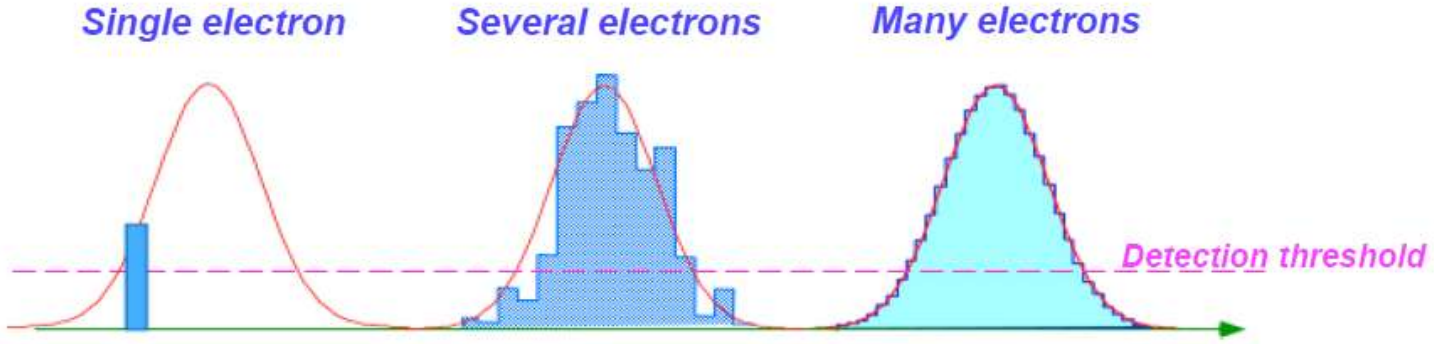

Error on first electron electron: $\sigma_1 \sim \frac{\pi}{2\sqrt{3\ln N}}\sigma_L$ **N=100** $\sigma_1 \sim 0.4\,\sigma_L$

RESOLUTION LIMITS OF DRIFT TUBES:

G. Scherberger et al, Nucl. Instr. and Meth. A424(1999)495
W. Riegler et al. Nucl. Instr. and Meth. A443(2000)156

LOCALIZATION ACCURACY IN DRIFT CHAMBERS

WORSENED BY LONG-RANGE ELECTRONS:

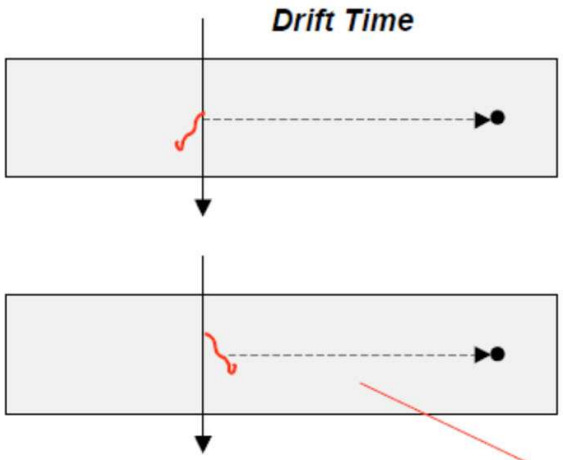

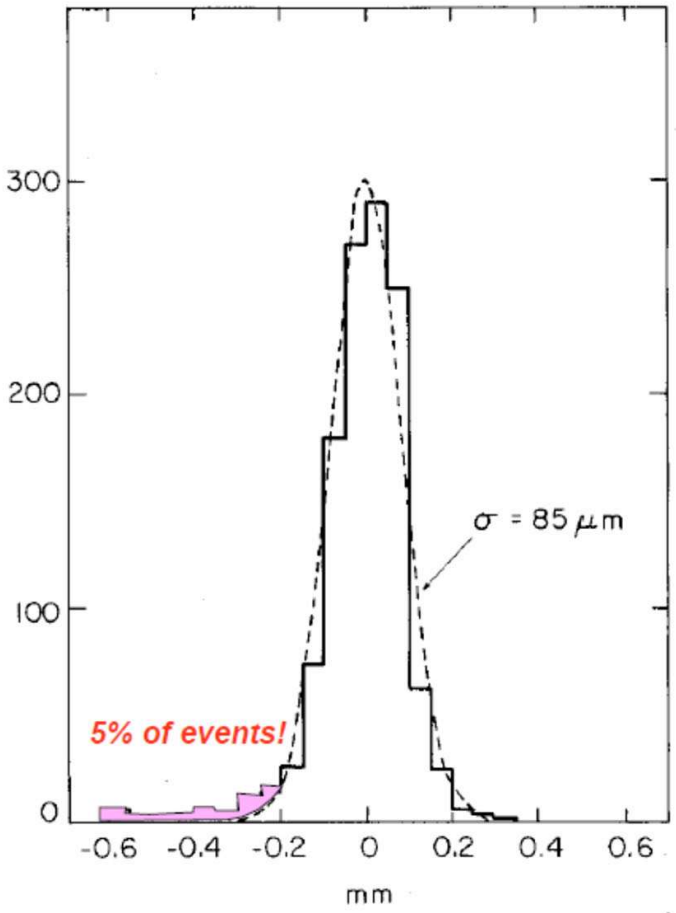

Time Projection Chambers (TPC)

Large volume active detector.

full 3-D track reconstruction

x-y from wires and segmented cathode of MWPC

z from drift time

and

dE/dx

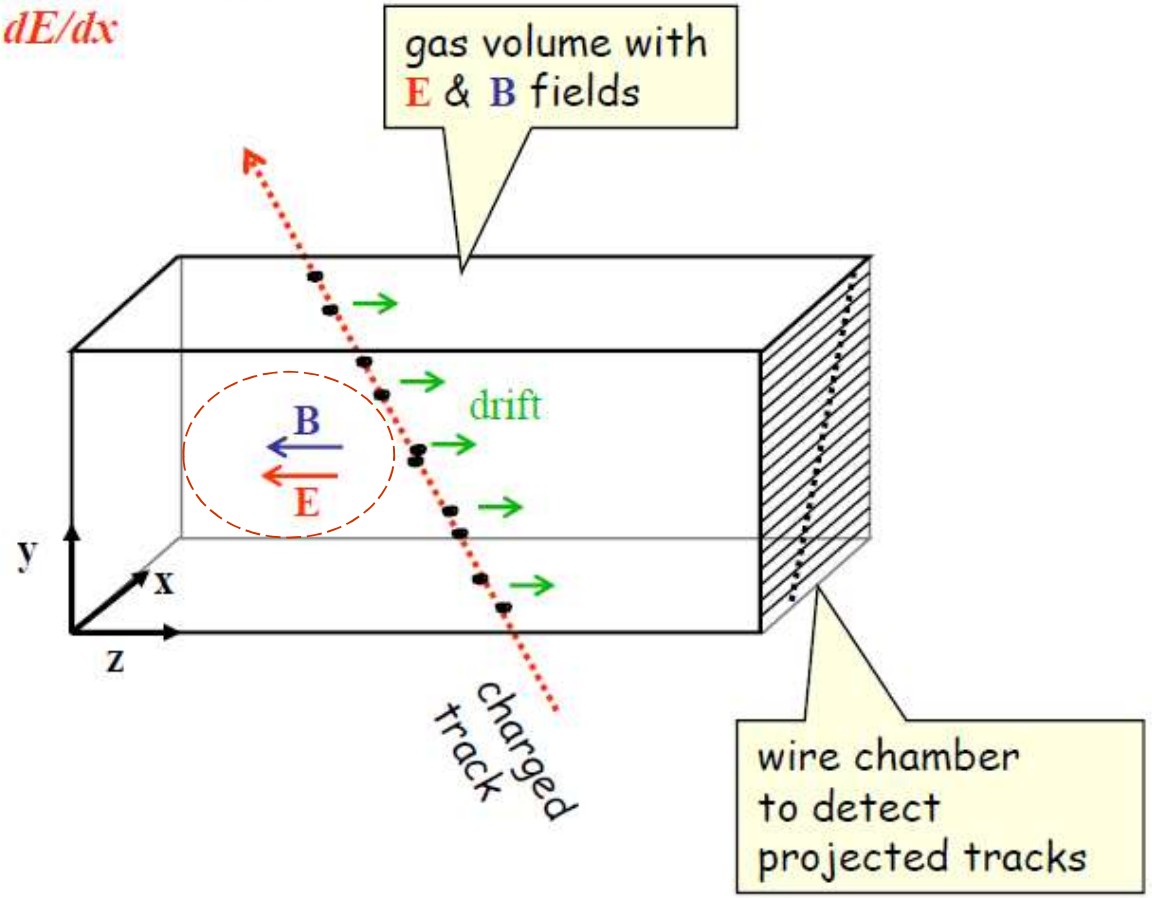

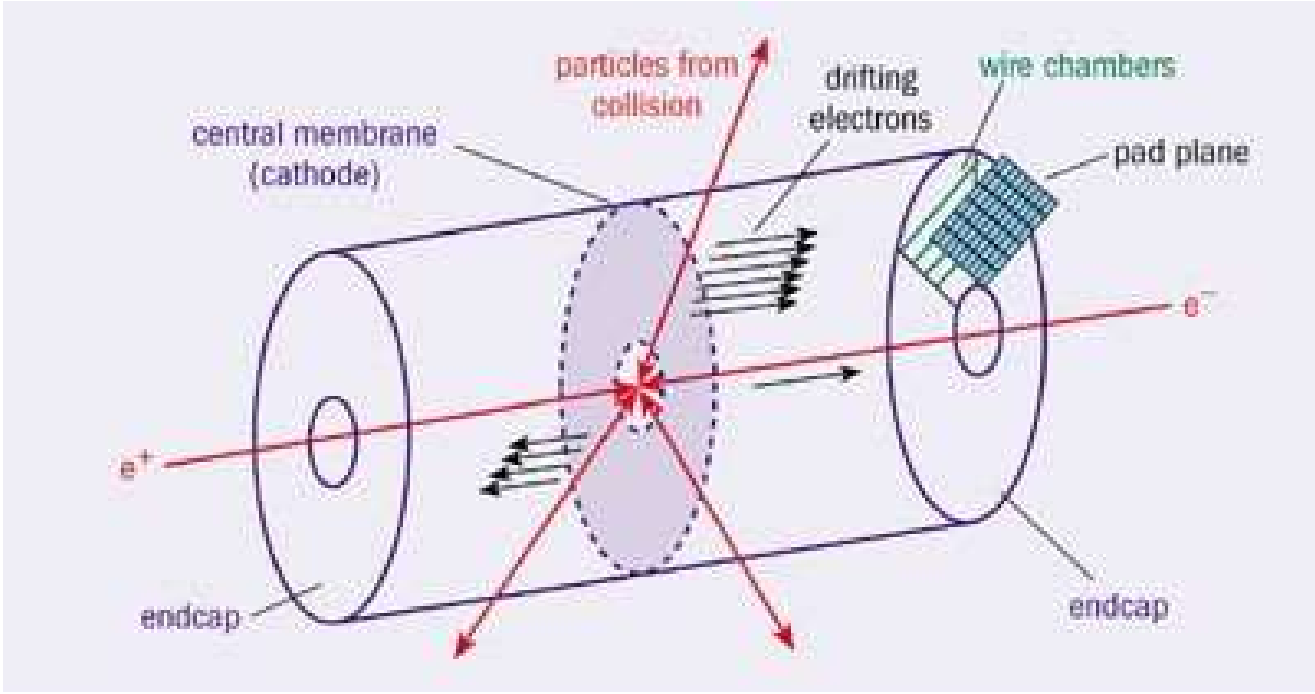
particles from collision
drifting electrons
wire chambers
central membrane (cathode)
pad plane
e⁻
e⁺
endcap
endcap

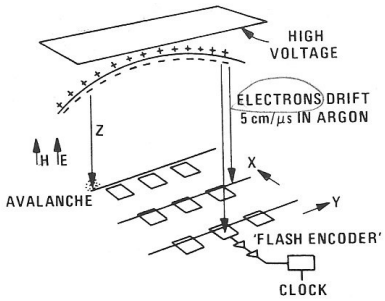

Fig. 6.18. Sampling the space points on a particle trajectory with the TPC (from *Lillberg* [6.31])

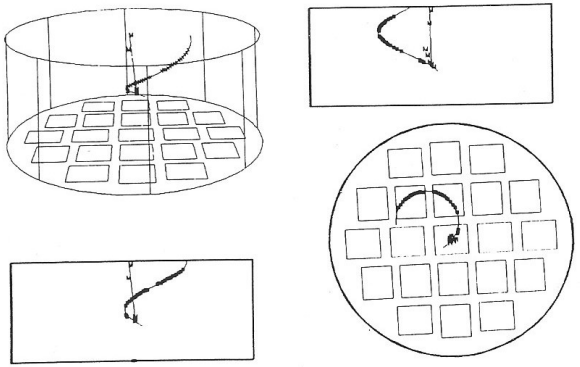

Fig. 6.19. Various views of TPC reconstructed tracks from an event in which an incident muon decays into a positron. The muon track is denoted by a *M* (from *Lillberg* [6.31])

TPC WORKING PRINCIPLE

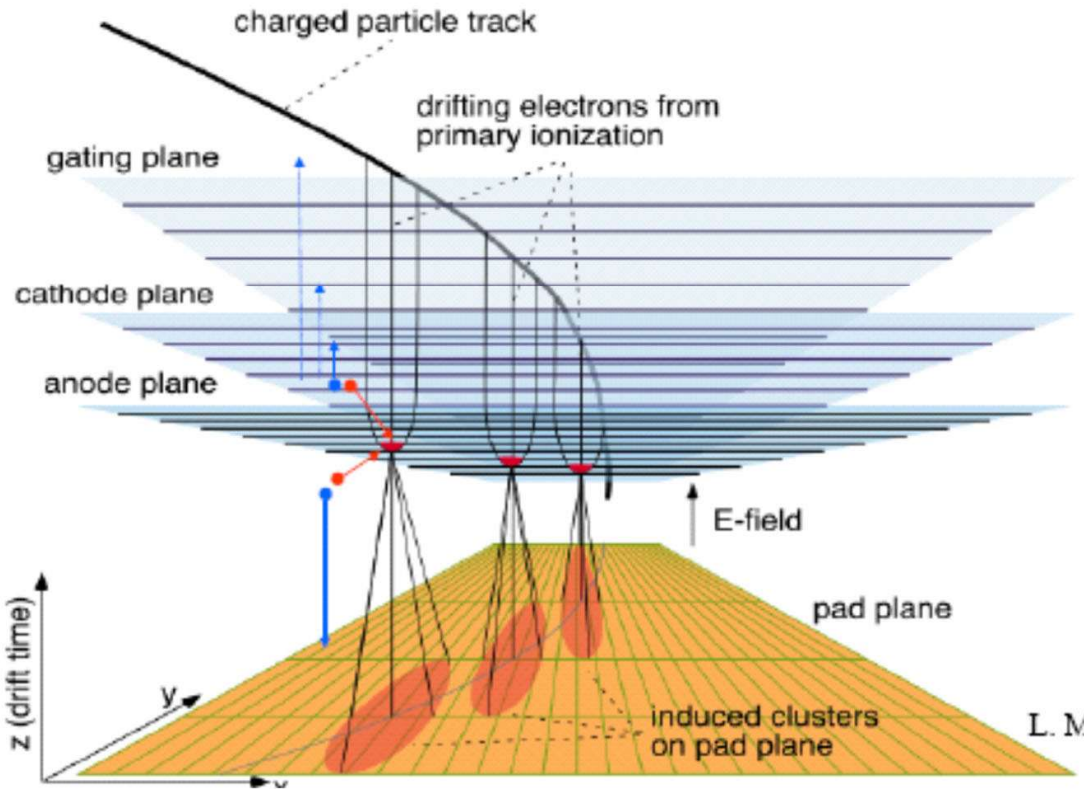

L. Musa, CERN

More on TPCs

Usually $B \parallel E$ improvement of diffusion
Drift length ≥ 1m
Rather (very) stringent requirement on homogeneity of E and B field
Space charge by ions
"Slow" detector

$$t_D \sim 10 \rightarrow 100\ \mu s$$

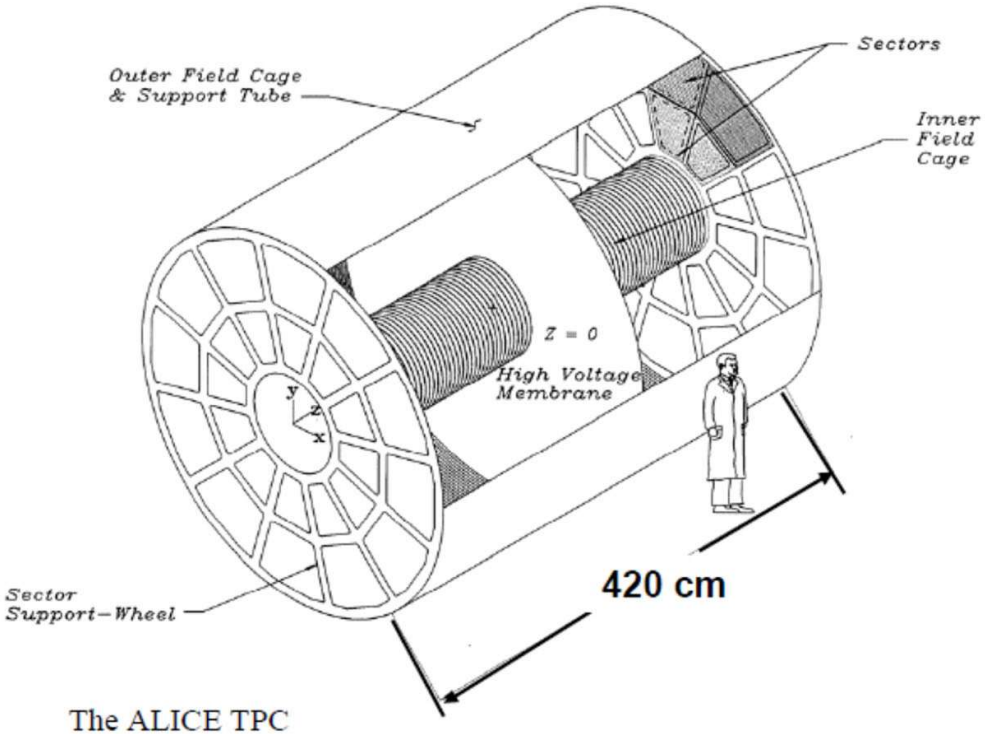

The ALICE TPC

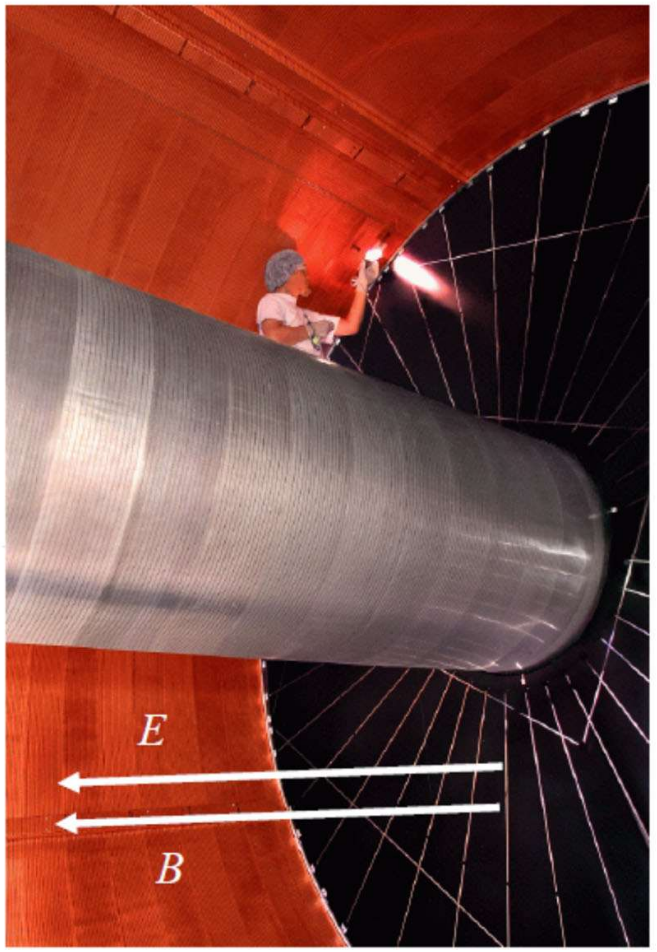

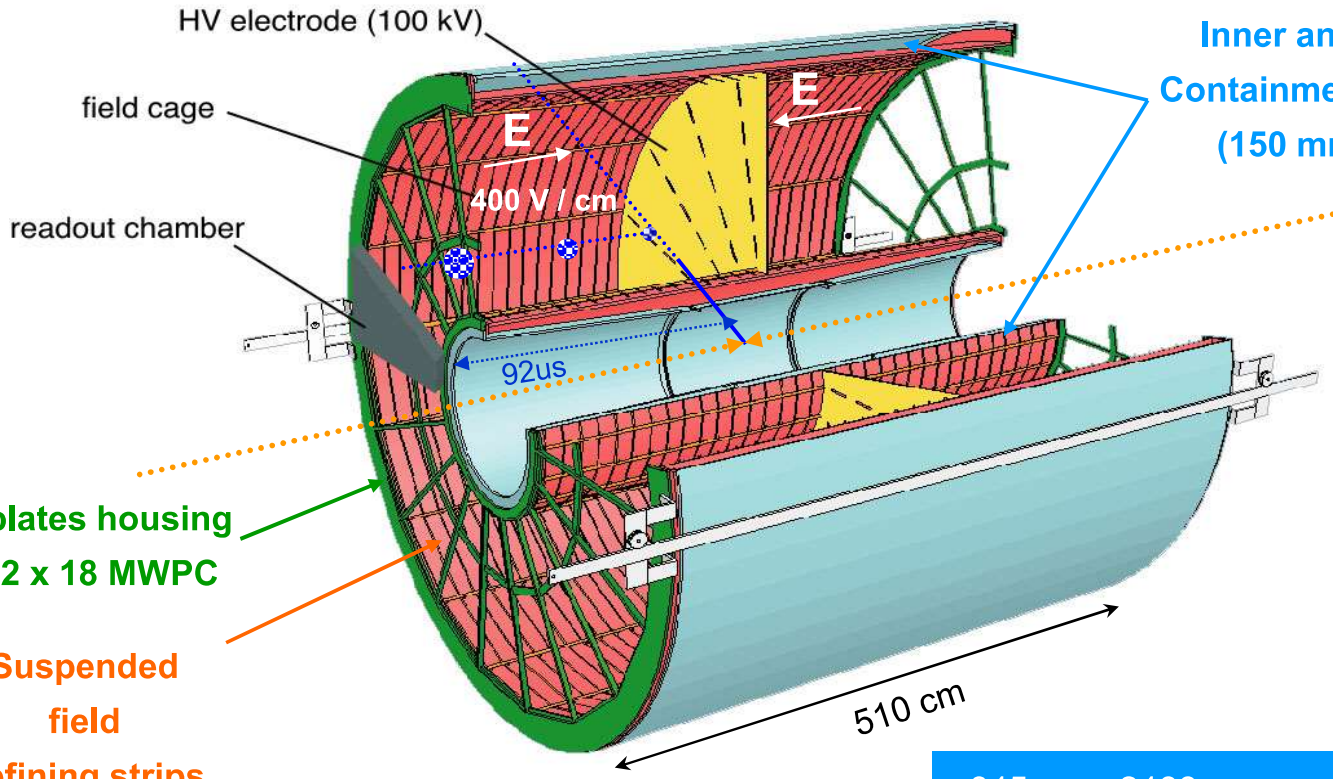

Inner and Outer Containment Vessels (150 mm, CO_2)

Endplates housing 2 x 2 x 18 MWPC

Suspended field defining strips 400 V / cm

ALICE TPC CHALLENGES

up to 2×10^4 charged particles in TPC

- 845 < r < 2466 mm
- drift length 2 x 2500 mm
- **drift gas Ne, CO_2, N_2 (90/10/5)**
- gas volume 95 m^3
- 557568 readout pads

High multiplicity Au + Au $\sqrt{S_{NN}}$ = 130 GeV (STAR TPC)

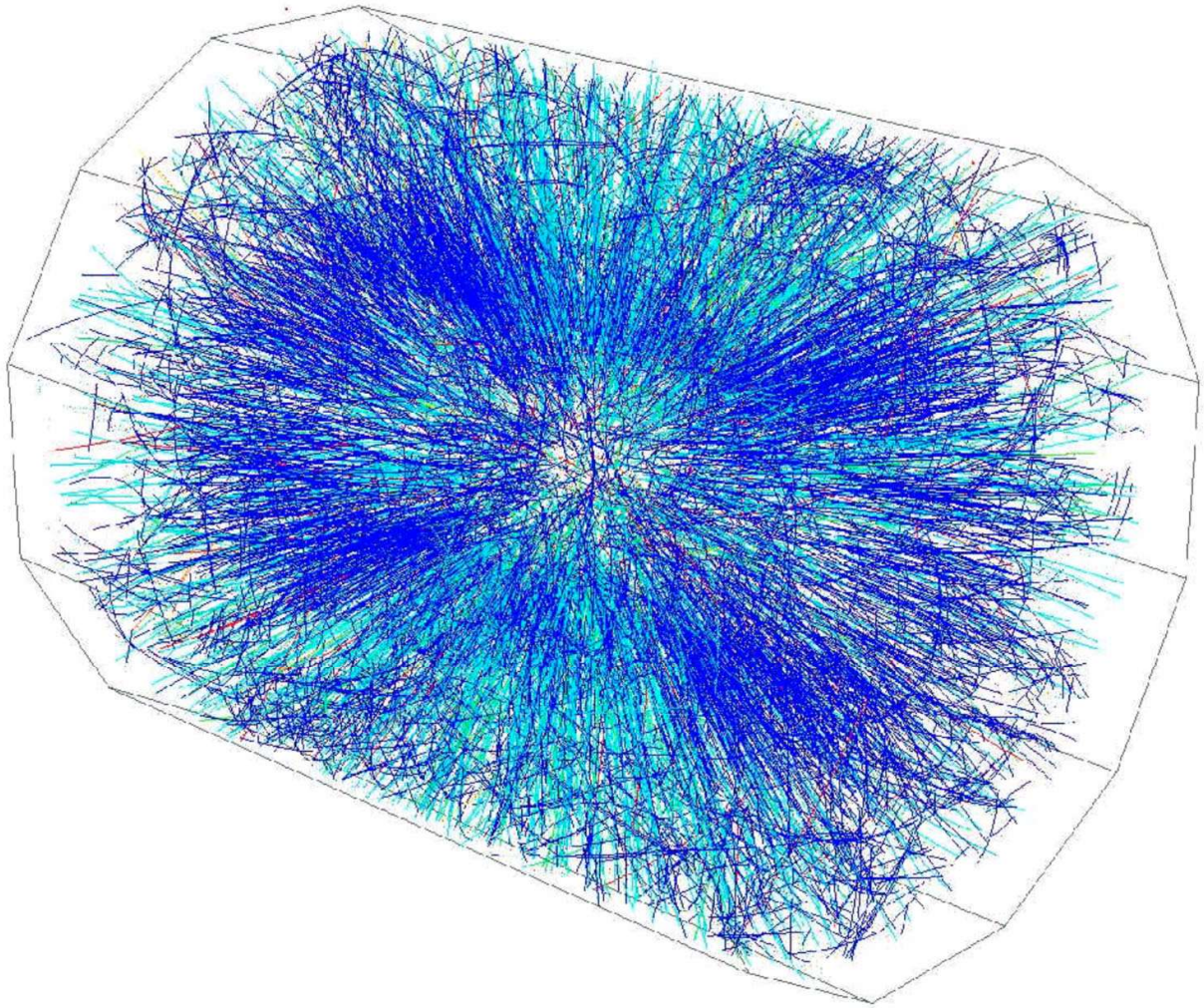

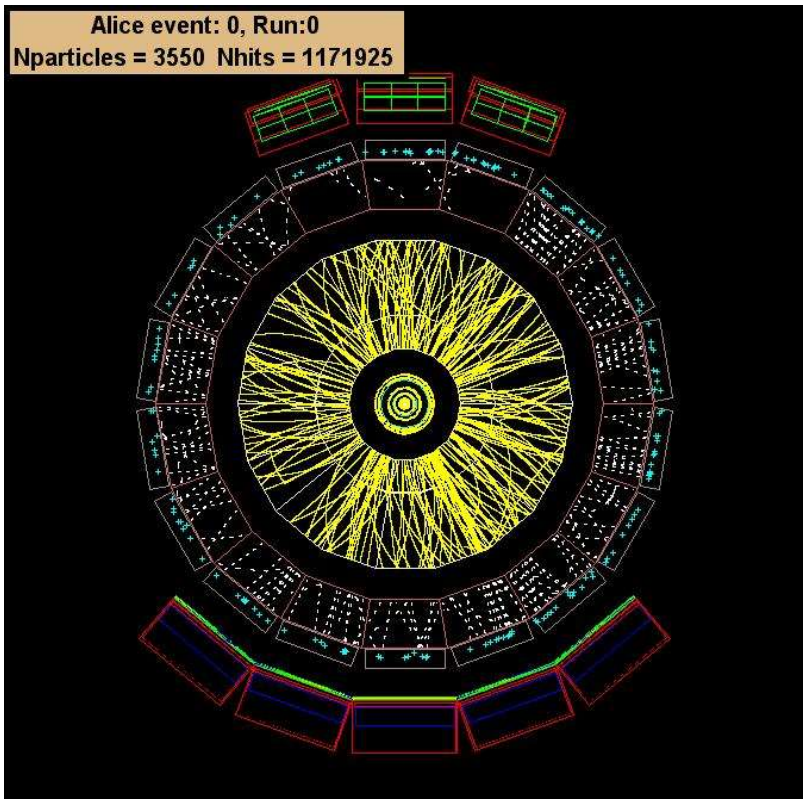

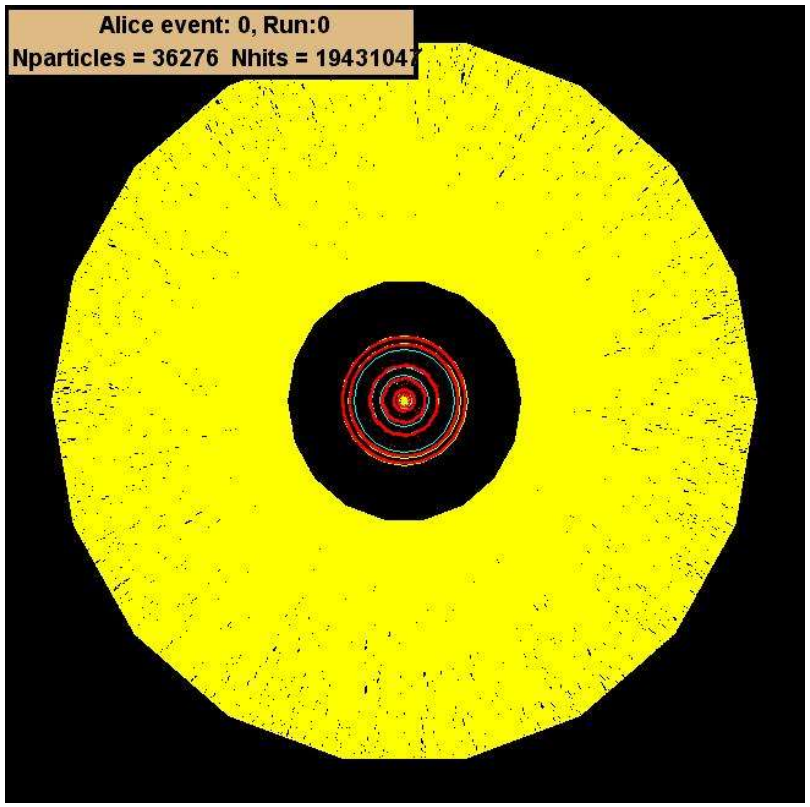

$60° < \vartheta < 62°$!

One collision :
Pb+Pb @ 5.5 TeV
dN/dy = 8,000